

BARE PCB INSPECTION BY MEAN OF ECT TECHNIQUE WITH SPIN-VALVE GMR SENSOR

K. Chomsuwan¹, S. Yamada¹, M. Iwahara¹, H. Wakiwaka², T. Taniguchi³, and S. Shoji⁴

¹ Kanazawa University, Kanazawa, Japan; ² Shishu University, Nagano, Japan;

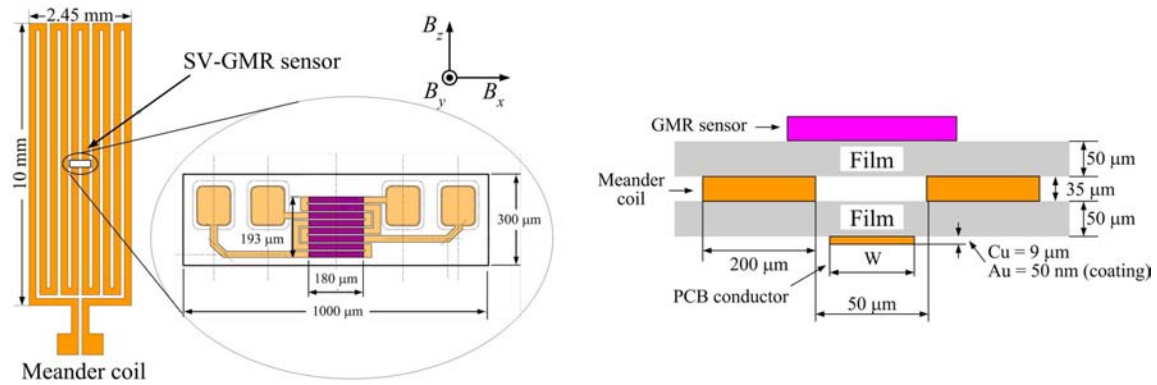
³ The University of Electro-Communications, Tokyo, Japan; ⁴ TDK corporation, Nagano, Japan;

Abstract: The high-sensitive micro eddy-current testing (ECT) probe composed of planar meander coil as an exciter and spin-valve giant magneto-resistance (SV-GMR) sensor as a magnetic sensor for bare printed circuit board (PCB) inspection is proposed in this paper. The high-sensitive micro ECT probe detects the magnetic field distribution on the bare PCB and the image processing technique analyzes output signal achieved from the ECT probe to exhibit and to identify the defects occurred on the PCB conductor. The inspection results of the bare PCB model show that the proposed ECT probe with the image processing technique can be applied to bare PCB inspection. Furthermore, the signal variations are investigated to prove the possibility of applying the proposed ECT probe to inspect the high-density PCB that PCB conductor width and gap are less than 100 μm .

Introduction: Eddy-current testing (ECT) technique is a well known method of non-destructive testing that is, usually, applied to evaluate the material flaws without changing or altering of testing material. Generally, ECT technique is used as crack detection in piping systems of nuclear power plants, as imperfect welding spot detection on aircrafts, and etc. In recent year, several kinds of magnetic sensors, such as Hall, Giant Magneto-resistance (GMR), Squid, and etc., have been successful in ECT technique for applying to nondestructive testing to detect material cracks. Especially, the GMR sensor is very interesting because it provides a good performance versus its cost. GMR sensor has high sensitivity over board range of frequency and high spatial resolution because it has small dimension [1, 5]. Moreover, it is inexpensive and able to operate at room temperature. From the features above, the applications of GMR sensor to ECT technique will provide the good inspection signals that can identify the defect points easily [1, 5].

Bare PCB inspection is a new application of ECT technique that has been proposed [1-4]. Many kinds of inspection technique, usually, are used for bare PCB inspection such as image scanning by CCD camera and conductive testing by pin probe. Image scanning method has an advantage because it is a non-contact method. However, this approach can inspect neither invisible short circuit nor disconnection. For conductive testing by pin probe, this approach is able to inspect the short circuit and disconnection whereas inspection of imperfection on PCB conductor can not be inspected. ECT technique is an interesting method for bare PCB inspection because this method likes the combination of the above methods. It means that ECT technique is a non-contact method and able to inspect not only conductor disconnections and short circuits but also partial defects on PCB conductor track width and thickness by eddy-current. Moreover, the construction of bare PCB inspection system by mean of ECT technique is uncomplicated and also inexpensive.

In this paper, bare PCB inspection characteristics of high-sensitive micro ECT probe composed of planar meander coil and SV-GMR sensor are proposed. Various methods of image processing technique have been developed to eliminate noise, enhance signal at defect points, and visualize 2-D image to represent bare PCB for defect identification [6-7]. In this paper, simple image processing technique is applied to recognize PCB defects easily. In addition, inspection of high-density PCB model with 100 μm PCB conductor width and gap is proposed.

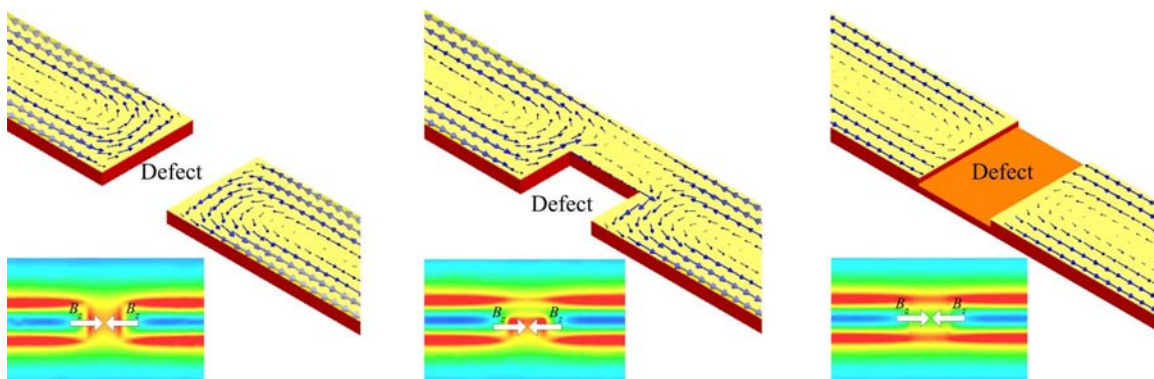


(a) Top view of ECT probe for PCB inspection and SV-GMR sensor. (b) Cross section of ECT probe to represent dimensions.

Fig.1 Configuration of the proposed ECT probe

Proposed ECT probe and principle: Configuration of the proposed ECT probe (Fig. 1) consists of a meander coil functioning as an exciting coil and a SV-GMR sensor functioning as a magnetic sensor. The high frequency alternating current, more than 5 MHz, is fed to the meander coil. Then, eddy-current is generated in the PCB conductor due to the high frequency excitation. The SV-GMR sensor with effective area of $180 \mu\text{m} \times 193 \mu\text{m}$ is mounted on the meander as shown in Fig.1 (a). Cross section of the proposed ECT probe as shown in Fig.1 (b) represents the dimension properties of the probe. Two films sandwich the meander coil to separate it from the SV-GMR sensor and the PCB conductor.

Normally, exciting current flows in the z -axis and also generates magnetic field density, B , in the x - and y - axis. Caused by high frequency excitation, the eddy-current generated in PCB conductor usually flows in the z - axis. The eddy-current will flow in the x -axis whenever PCB defect or soldering point is detected. Therefore, the magnetic field density, B , in the z -axis is generated. For PCB defect detection, the magnetic sensor was mounted on the meander coil to detect only the magnetic field density, B , in the z -axis. Fig. 2 shows the eddy-current paths and magnetic field density over the PCB conductor achieved from finite element analysis. PCB conductor, $100 \mu\text{m}$ width, with $50 \mu\text{m}$ conductor disconnection was used in the simulation. As high frequency excitation, the eddy-current density near the boundary of the PCB conductor is higher than the density in other area. Consequently, the magnetic field density, B , will concentrate at the boundary region of the PCB conductor. In case of PCB conductor imperfection, two types of defect model were used in the simulation. First is the partial defect on PCB conductor width that the defect width was allocated only 50% of PCB conductor width. Second is the partial defect on PCB conductor thickness that the defect thickness was allocated only 50% of PCB conductor thickness. From the simulation results, magnetic field density B_z occurring over the partial defect in thickness of PCB conductor is low because low eddy-current flows.



(a) Disconnection

(b) Partial defect in width

(c) Partial defect in thickness

Fig. 2 Eddy-current path and magnetic field density over the PCB conductor with conductor disconnection and imperfection on PCB conductor

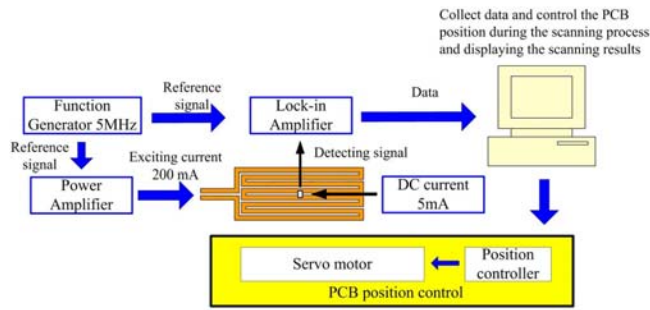


Fig. 3 Configuration of the proposed bare PCB inspection system based on ECT technique

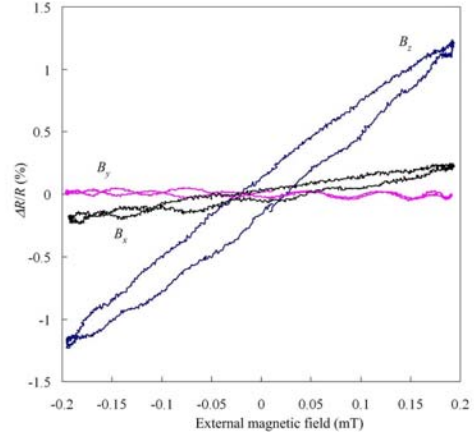


Fig. 4 SV-GMR sensor characteristics at each of its axes

Results: The configuration of the proposed bare PCB inspection system is shown in Fig.3. Because PCB conductor with 9 μm thickness made from CU coated by 0.05 μm AU was used as model in the experiment, sinusoidal current of 200 mA at frequency of 18 MHz was fed to the meander coil to enable the inspection of the PCB conductor with less than 10 μm thickness. A normal resistance of SV-GMR sensor used in this experiment is 630 Ω . The SV-GMR sensor has maximum MR ratio around 10.37 %. As shown in Fig. 4, the sensitivity, in the range of $\pm 200 \mu\text{T}$, of the SV-GMR sensor only in sensing axis is around 6 %/mT whereas that in the other axes is less than 1 %/mT. DC bias current of 5 mA was fed to SV-GMR sensor. Lock-in amplifier, Stanford SR 844 model, was used to measure voltage drop across SV-GMR sensor. The PCB conductor widths are 500, 300, 200, 100, and 70 μm that were used as bare PCB model in the experiment. Therefore, scanning pitch was set at 20 μm to achieve accurate results and ECT probe scanned over PCB only in horizontal direction (parallel to the PCB conductor).

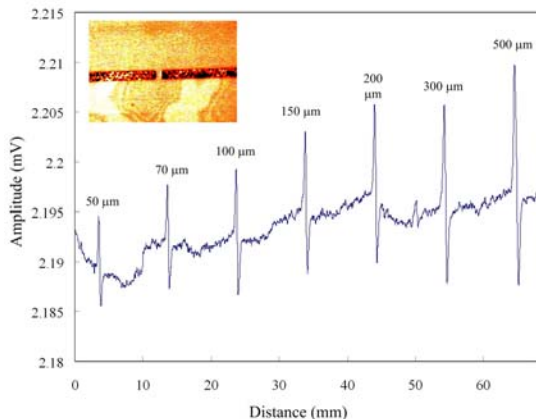


Fig. 5 Inspection signal obtained from scanning

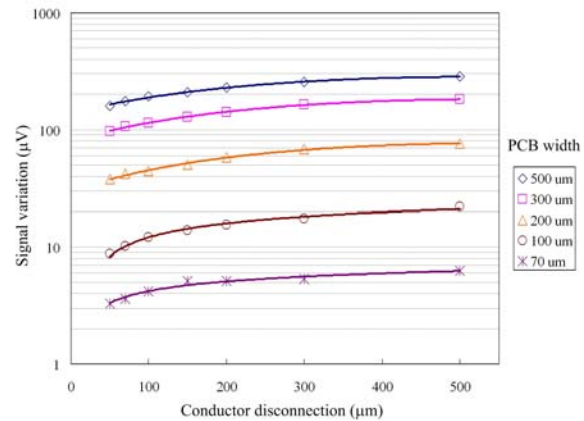


Fig. 6 Signal variations versus conductor

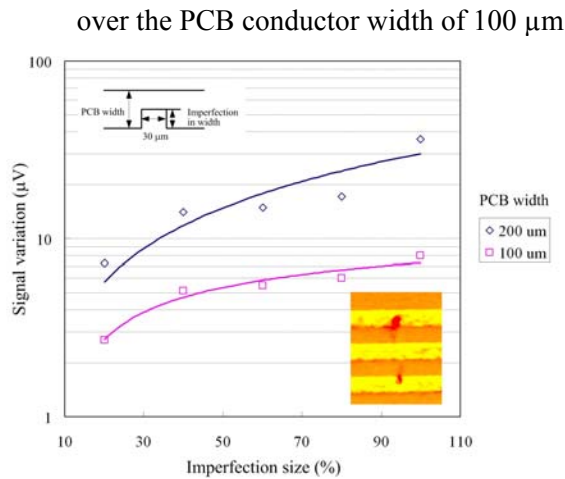


Fig. 7 Signal variations versus partial defects on PCB conductor track widths

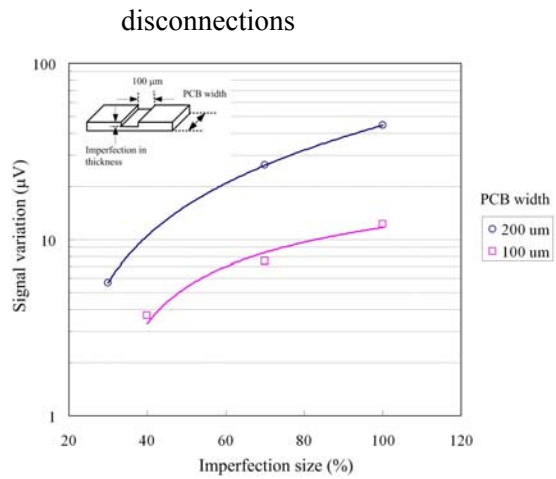


Fig. 8 Signal variations versus partial defects on PCB conductor thicknesses

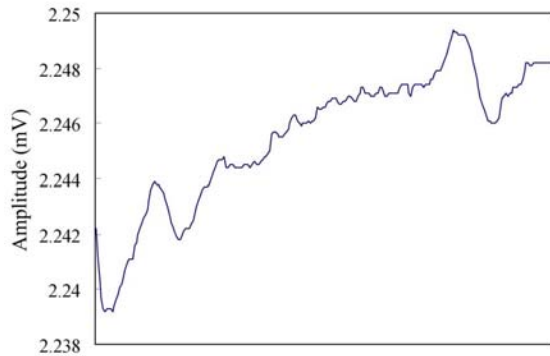
Inspection signals at each of defect points have same pattern but different magnitude as shown in Fig. 5. SV-GMR sensor can detect low magnetic field variation that, usually, occurs at defect or boundary of PCB conductor. Low signal variation will occur at small defect point whereas high signal variation will be found at large defect point. Moreover, the PCB conductor size effect to the signal variation at defect point as shown in Fig. 6. For example, the signal variations obtained from the PCB conductor with conductor width of 500 μm are bigger than that from the PCB conductor with conductor width of 70 μm around 600%. Imperfection on PCB conductor track width and thickness can be also inspected by the proposed ECT probe. Fig. 7 and Fig. 8 show the signal variations at the partial defects on PCB conductor track width and thickness respectively. PCB conductors with 200 μm and 100 μm conductor width were used as model for the partial defect inspection. The defect width was fixed at 30 μm for PCB conductor imperfection on track width and 100 μm for PCB conductor imperfection on thickness. The signal variations at partial defect are lower than the signal variations at conductor disconnection. The signal variations occurred at thickness defect is very small as mentioned above. However, it is large enough to specify the defect points.

Image processing technique: Usually, ECT signals obtained from scanning over bare PCB contain undesired components, such as noise, offset, and etc., that cause wrong recognition of PCB defects. Therefore, image processing technique is necessary to eliminate undesired signal and to enhance the information at the defects to achieve effective defect identification. In this paper, the simple image processing technique was applied because it provides satisfied results. Four steps of the image processing are following:

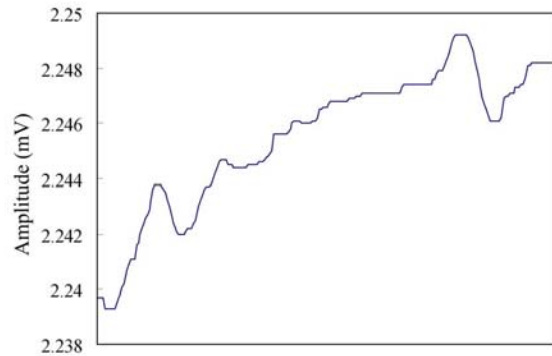
- 1) Removal of noise from ECT signals by median filtering
- 2) Elimination of offset and enhancement of the signals at defect point by numerical gradient
- 3) Removal of noise by 5×5 median filter and visualization of the 2-D image to represent bare PCB
- 4) Comparison between the 2-D image bare PCB model and non-defect 2-D image PCB model to identify the defect points

Fig. 9 (a) and (b) show the ECT signals obtained by scanning over the PCB conductor and ECT signals after median filtering was applied respectively. One dimension median filtering was chosen for this proposed because it is able to smoothing of signals, suppression of impulse noise, and preserving of edge and is not difficult to implement. From Fig. 9 (c), the ECT signals after filtering were visualized to represent the 2-D image of bare PCB model. However, 2-D image is not clear enough to specify the defects because of difference offsets of ECT signals. One dimension numerical gradient technique was applied to eliminate the offsets and to enhance the

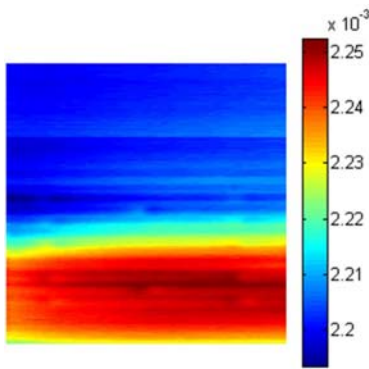
signals at the defects because this technique is very simple and faster than other methods such as wavelet-based technique. 2-D image after applying the numerical gradient method is shown in Fig. 9 (d). The signals at defect points are not clear enough because the numerical gradient technique is also sensitive to noise. Therefore, 5×5 median filtering is applied to eliminate noise before visualizing the 2-D image to represent the bare PCB model as shown in Fig. 9 (e). Therefore, identification of PCB defects by comparing with the 2-D image of non-defect PCB model is not difficult.



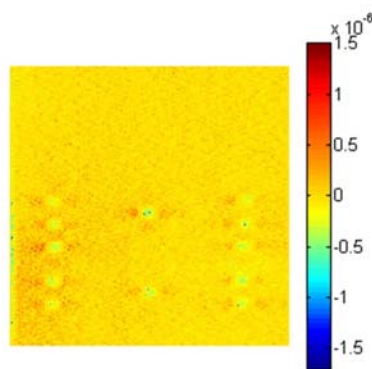
(a) ECT signal obtained from measurement



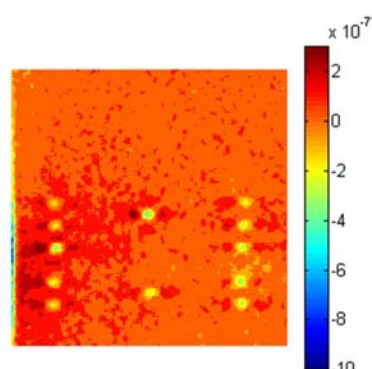
(b) ECT signal after median filtering



(c) 2-D image after filtering

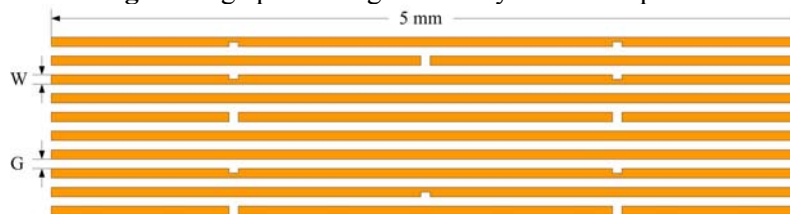


(d) 2-D image after gradient

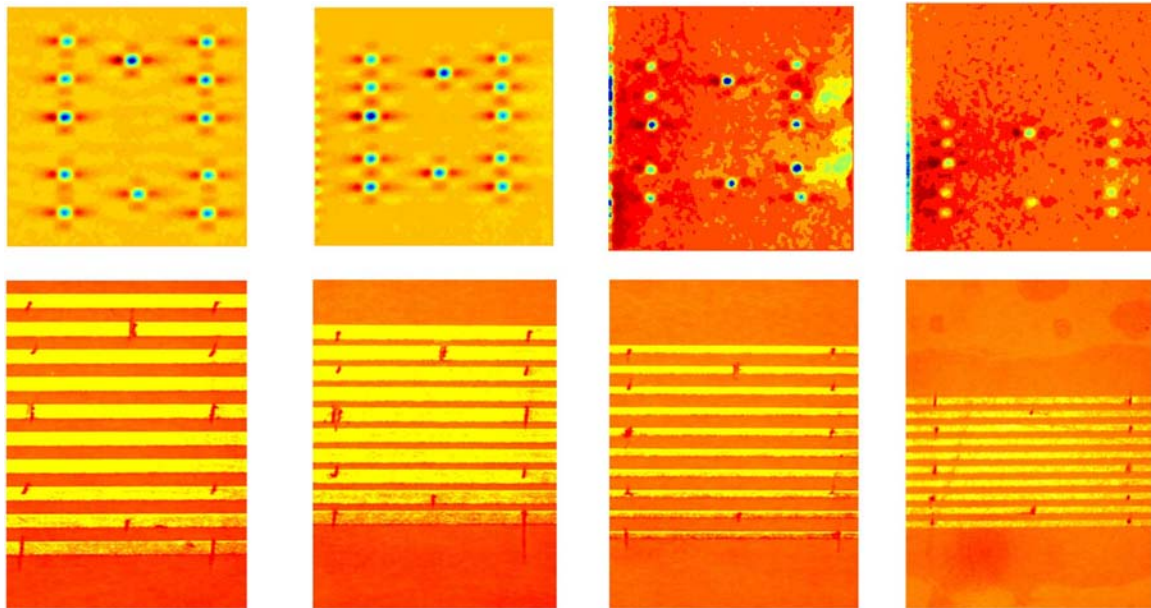


(e) 2-D image after filtering

Fig. 9 Image processing to identify the defect points



(a) PCB model



(b) $W = 200 \mu\text{m}$,
 $G = 200 \mu\text{m}$

(c) $W = 200 \mu\text{m}$,
 $G = 100 \mu\text{m}$

(d) $W = 100 \mu\text{m}$,
 $G = 200 \mu\text{m}$

(e) $W = 100 \mu\text{m}$,
 $G = 100 \mu\text{m}$

Fig. 10 PCB models and inspection results

Discussion: As shown in Fig. 10 (a), ten lines of PCB conductor with different conductor width, W , and gap, G , was used as model. The bare PCB model was identified to four models as following:

- 1) $200 \mu\text{m}$ PCB conductor width, W , with $200 \mu\text{m}$ gap, G
- 2) $200 \mu\text{m}$ PCB conductor width, W , with $100 \mu\text{m}$ gap, G
- 3) $100 \mu\text{m}$ PCB conductor width, W , with $200 \mu\text{m}$ gap, G
- 4) $100 \mu\text{m}$ PCB conductor width, W , with $100 \mu\text{m}$ gap, G

Fig 10 (b)-(e) present the PCB pictures and scanning results after image processing was applied. The same defects were allocated on the PCB model. The smallest conductor disconnection was only $20 \mu\text{m}$. Furthermore, different kinds of partial defects were located on this model. The scanning results present that the proposed probe is able to inspect the defects on the PCB conductor. 2-D image of bare PCB inspection with $200 \mu\text{m}$ track width as shown in Fig. 10 (b) and (c) has low noise. Therefore, it is easy to specify the defects although the gap of PCB conductor model is small ($100 \mu\text{m}$). From inspection results of the bare PCB with $100 \mu\text{m}$ track width as shown in Fig. 10 (d) and (e), the defects on PCB conductor are still not difficult to identify although the images are not clear like the inspection of PCB conductor with $200 \mu\text{m}$ width. The signals obtained from the inspection of PCB conductor with $200 \mu\text{m}$ width provide high signal variations at defect point more than the signals from inspection of PCB conductor with $100 \mu\text{m}$ width as mentioned above. PCB conductor gap is one of parameters that effect to the signal variations. Signal variations at defect point become low when the gap between PCB conductors is small if spatial resolution of SV-GMR sensor is not high enough. For this proposed, increasing of spatial resolution, therefore, is needed for inspection of high density PCB that is less than $100 \mu\text{m}$ gap.

Conclusions: The high-sensitive micro ECT probe consisted of planar type exciting coil and SV-GMR sensor was applied to inspection of defects on PCB conductor. High-frequency exciting current, 18 MHz , fed to the exciting coil make a possibility to inspect the defects on very thin PCB conductor, less than $10 \mu\text{m}$. Not only conductor disconnection but also imperfection on PCB conductor can be detected. Furthermore, the experimental results provide the possibility of inspection of high-density PCB that has gap between PCB conductors less than $100 \mu\text{m}$. In order

to identify the defect points, applying of simple image processing technique is able to recognize the defect points easily. Therefore, bare PCB inspection by ECT technique is an alternative way to achieve the accurate results.

Acknowledgment: This work was supported in part by a Grand-in-Aid for Scientific Research from Japan Society for Promote of Science (Category B, 14350218)

References:

- [1] K. Chomsuwan, Y. Fukuda, S. Yamada, M. Iwahara, H. Wakiwaka, and S. Shoji, "GMR Sensor Utilization for PCB Inspection Based on the Eddy-Current Testing Technique," *Transaction on the Magnetic Society of Japan*, Vol. 4, No.1, pp. 39-42, February 2004.
- [2] S. Yamada, M. Iwahara, Y. Fukuda, T. Taniguchi, and H. Wakiwaka, "Inspection of Bare Printed Circuit Board Using Planar Type ECT probe," *Review of Quantitative Nondestructive Evaluation*, Vol. 23, pp. 374-381, 2004.
- [3] S. Yamada, K. Nakamura, M. Iwahara, T. Taniguchi, and H. Wakiwaka, "Application of ECT technique for Inspection of Bare PCB," *IEEE Transactions on Magnetics*, Vol. 39, No. 5, pp 3325-3327, September 2003.
- [4] D. Kacqszak, T. Taniguchi, N. Nakamura, S. Yamada, and M. Iwahara, "Novel eddy current testing sensor for the Inspection of Printed Circuit Boards," *IEEE Transactions on Magnetics*, Vol. 37, No. 4, pp. 2010-2012, July 2001.
- [5] T. Dogaru and S. T. Smith, "Giant Magnetoresistance-Based Eddy-Current Sensor," *IEEE Transactions on Magnetics*, Vol. 37, No. 5, pp. 3831-3838, September 2001.
- [6] T. Taniguchi, D. Kacqszak, S. Yamada, and M. Iwahara, "Wavelet-Based Processing of ECT Images for Inspection of Printed Circuit Board," *IEEE Transactions on Magnetics*, Vol. 37, No. 4, pp. 2790-2793, July 2001.
- [7] T. Taniguchi, D. Kacqszak, S. Yamada, M. Iwahara, and T. Miyagoshi, "Defect Detection of Printed Circuit Board by Using Eddy-Current Testing Technique and Image Processing," *Electromagnetic Nondestructive Evaluation (IV)*, pp. 111-119, 2000.